Negative Poisson's ratios as a common feature of cubic metals

Ray H. Baughman*, Justin M. Shacklette*, Anvar A. Zakhidov* & Sven Stafström†

** AlliedSignal Inc., Research and Technology, Morristown, New Jersey 07962-1021, USA*
† Department of Physics and Measurement Technology, Linköping University, S-581 83, Linköping, Sweden

Poisson's ratio is, for specified directions, the ratio of a lateral contraction to the longitudinal extension during the stretching of a material. Although a negative Poisson's ratio (that is, a lateral extension in response to stretching) is not forbidden by thermodynamics, this property is generally believed to be rare in crystalline solids[1]. In contrast to this belief, 69% of the cubic elemental metals have a negative Poisson's ratio when stretched along the [110] direction. For these metals, we find that correlations exist between the work function and the extremal values of Poisson's ratio for this stretch direction, which we explain using a simple electron-gas model. Moreover, these negative Poisson's ratios permit the existence, in the orthogonal lateral direction, of positive Poisson's ratios up to the stability limit of 2 for cubic crystals. Such metals having negative Poisson's ratios may find application as electrodes that amplify the response of piezoelectric sensors.

There is considerable fundamental and practical interest in materials with negative Poisson's ratios[1–14], which Evans[4] called auxetic. We refer to auxetic crystals as axially auxetic or non-axially auxetic, depending upon whether or not a negative Poisson's ratio arises for a crystal-axis direction. The calculation of Poisson's ratio is complicated for directions oblique to the crystal axes, because the elastic constant tensor for general orientations involves as many as 21 interrelated components for even a cubic phase[15]. This complication probably explains why the common existence of non-axial auxetic behaviour has largely remained unrecognized. However, the important early work of Milstein and Huang[16] established the occurrence of non-axial auxetic behaviour for cubic metals and rare gases. The origin of this behaviour must differ from that of other known types of auxetic materials and structures: foams, honeycombs and hypothetical carbon phases having re-entrant or hinged structures[2–5,8,13]; microporous organic polymers[4]; polymer laminates[11,14]; polymer/fibre composites[12]; and crystals such as α-cristobalite[1,6].

We simplify the search for auxetic materials by deriving a general criterion for the existence of auxetic behaviour. This 'auxetic criterion', expressed in elastic compliances (S_{ij}) for the axial directions, is that $S_{11} + S_{33} + 2S_{13} - S_{44} > 0$. Satisfying this inequality is a necessary and sufficient condition for auxetic behaviour for a hexagonal or cubic phase when the Poisson's ratios for axial directions are all positive. This general criterion is derived from equations for the Poisson's ratio for an arbitrary direction for cubic[15] and hexagonal[17] phases. Using these equations, the Poisson's ratios that usually have extremal values for cubic phases are:

$$\nu(110, 1\bar{1}0) = -(2C_{11}C_{44} - (C_{11} - C_{12})(C_{11} + 2C_{12}))/(2C_{11}C_{44} + (C_{11} - C_{12})(C_{11} + 2C_{12})) \quad (1)$$

$$\nu(110, 001) = 4C_{12}C_{44}/(2C_{11}C_{44} + (C_{11} - C_{12})(C_{11} + 2C_{12})) \quad (2)$$

These are the Poisson's ratios for a [110] stretch, measured for [1$\bar{1}$0] and [001] lateral directions, respectively. Such Poisson's ratios are for a stretch along the face diagonal of the cubic cell and a resulting lateral strain measured along a perpendicular face-diagonal and a perpendicular cube-axis direction, respectively.

We identified non-axial auxetic behaviour by the application of the above criterion to experimentally determined elastic compliance matrices (see ref. 18 and references therein, and Supplementary Information). About 69% of the 32 investigated cubic phases of the elemental metals satisfy the auxetic criterion. Of these 18 face-centred cubic (f.c.c.) metals and 14 body-centred cubic (b.c.c.) metals, 78% and 57%, respectively, are non-axially auxetic. For all of these cubic phases, except lithium, both the minimum and the maximum Poisson's ratio are for a [110] applied stress. In contrast, out of 20 investigated hexagonal close-packed (h.c.p.) phases, only

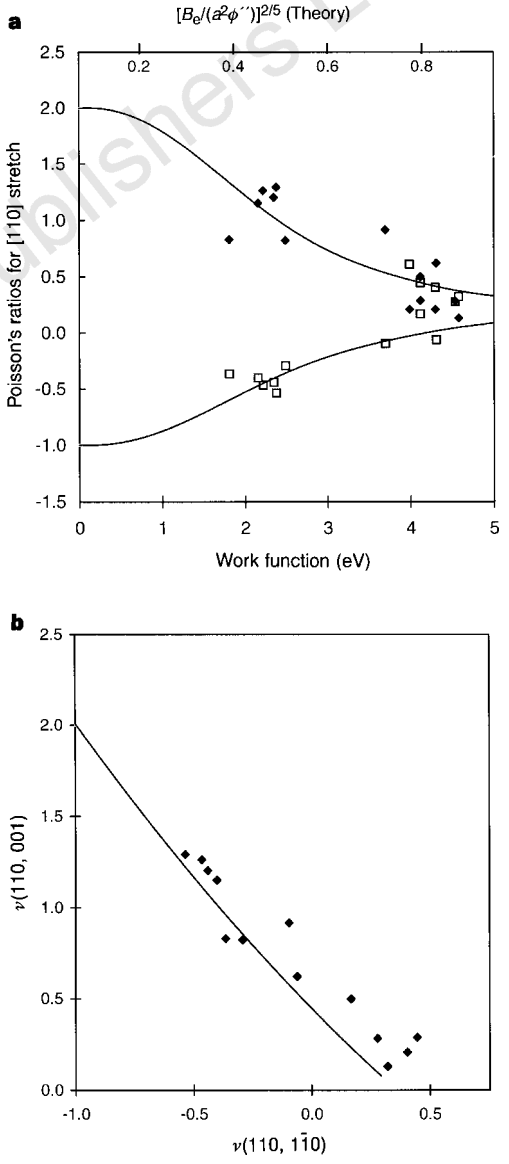

Figure 1 Correlations for the Poisson's ratios of b.c.c. metals, derived from observed[18,22] elastic compliances and polycrystalline work functions. **a**, Correlation between $\nu(110, 1\bar{1}0)$ and $\nu(110, 001)$ and the polycrystalline work function. The experimentally derived Poisson's ratios are denoted by unfilled squares for $\nu(110, 1\bar{1}0)$ and filled diamonds for $\nu(110, 001)$. The curves are predicted dependencies of $\nu(110, 1\bar{1}0)$ and $\nu(110, 001)$ (bottom and top curves, respectively) on $[B_e/(a^2\Phi'')]^{2/5}$; see text for details. **b**, Comparison of experimentally derived data points relating $\nu(110, 1\bar{1}0)$ and $\nu(110, 001)$ with the theoretical prediction (solid curve) for the simple two-term lattice energy used to obtain the theoretical curves of **a**.

zinc and beryllium are auxetic. Other than zinc, none of these cubic and hexagonal phases of elemental metals has a reliably reported negative Poisson's ratio for an axial direction. These results indicate for the elemental metals that (1) f.c.c. and b.c.c. phases are usually auxetic in non-axial directions, (2) axial auxetic behaviour is rare (or non-existent) for the cubic phases, and (3) the hexagonal phases are rarely auxetic for either axial or non-axial directions. None of the cubic phases are auxetic for a stretch along the three-fold axis direction, which is also the case for the auxetic trigonal phases of arsenic and bismuth characterized by Gunton and Saunders[19].

Our analysis of reported elastic compliance data for cubic alloys and the cubic intermetallic phases[18] provides results consistent with the above conclusions. Although none of the ~130 investigated cubic alloy and cubic intermetallic phases are auxetic for axial directions, ~50% of these phases are auxetic for non-axial directions. Furthermore, all those cubic alloy and cubic intermetallic phases that are auxetic contain at least one element that has an auxetic phase, and auxetic behaviour is almost always found for such cubic phases that contain only elements having auxetic phases.

In contrast with these results for metals, application of the auxetic criterion to published elastic compliance matrices[18] shows that auxetic behaviour of any type is either rare or non-existent for many classes of cubic materials. For example, all investigated cubic alums (48 phases) and garnets (20 phases) are non-auxetic. Also, auxetic behaviour is rare or non-existent for salts with either the NaCl or the CsCl type structure. The diamond structural types for carbon, silicon and germanium are also non-auxetic. However, various cubic solids that share the ball-like packing of the elemental metals are auxetic. For example, non-axial auxetic behaviour is found[16,18,20,21] for the f.c.c. phases of rare gases, methane, ammonia and adamantane (but not for the f.c.c. phase of C_{60}).

The existence of negative Poisson's ratios for the cubic metals enables the existence of Poisson's ratios above unity. In fact, our analysis of the literature data[18] for metallic cubic phases provides non-axial Poisson's ratios that range between −0.67 and 1.47 for $Cu_{68.6}Al_{27.6}Ni_{3.8}$ and between −0.81 and 1.68 for $CuAuZn_2$. Also, ~20% of the ~80 investigated types of cubic alloys provide a maximum Poisson's ratio of above unity. Such metals must have a negative Poisson's ratio for the same stretch direction as the maximum Poisson's ratio (ν_{max}), otherwise the linear compressibility would be negative (thereby violating a stability condition for cubic phases). The existence of a $\nu_{max} > 1$ implies that a plane exists parallel to the stretch axis that decreases area during stretching. The most negative fractional area change ($\Delta A/A$) caused by a fractional elongation of $\Delta L/L$ is then $\Delta A/A = (1 - \nu_{max})\Delta L/L$.

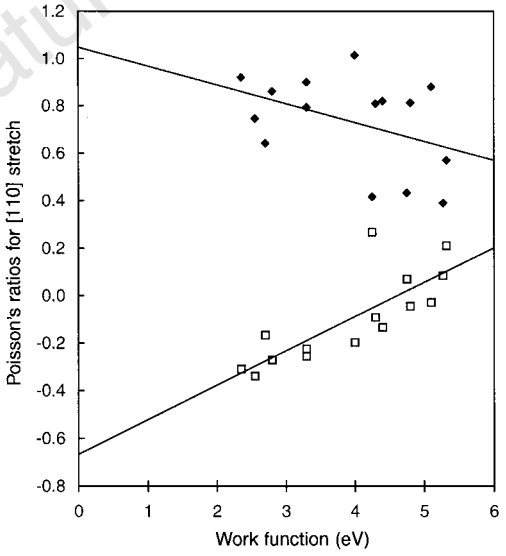

Figure 2 The dependence of $\nu(110, 1\bar{1}0)$ and $\nu(110, 001)$ on polycrystalline work function for f.c.c. phases of the non-ferromagnetic elemental metals. Unfilled squares denote $\nu(110, 1\bar{1}0)$ and filled diamonds denote $\nu(110, 001)$. The lines are least-squares fits to the experimental results, which are derived from reported compliances[18] and work functions[22].

Figures 1 and 2 show results that can be used both to understand the origin of the negative Poisson's ratios and to design new auxetic phases. These figures for b.c.c. metal phases (Fig. 1a) and for non-ferromagnetic f.c.c. metal phases (Fig. 2) show that the extremal Poisson's ratios for a [110] stretch are correlated with the measured work function[22]. We also find that correlations exist between either $\nu(110, 1\bar{1}0)$ or $\nu(110, 001)$ and $(n_{ws})^{1/3}$, $(H_{vap}/(V_M)^{2/3})^{1/3}$ and $V_M^{-1/3}$, where n_{ws} is the Wigner–Seitz electron density parameter[23], H_{vap} is the molar heat of vaporization, and V_M is the molar volume. These relationships reflect the correlation between off-axis Poisson's ratios and work function, as it is known[23] for metals that $(n_{ws})^{1/3}$, $(H_{vap}/(V_M)^{2/3})^{1/3}$ and $V_M^{-1/3}$ are correlated with work function.

We find that a simplistic model provides insight into the origin of the negative Poisson's ratios and the observed correlations. We approximate the energy per atom (U) of a crystal (with molar volume V and equilibrium molar volume V_o) by the sum of nearest-neighbour central force interactions (Φ) and a term that depends on the mth power of volume. The second derivative of this second term with respect to V/V_o (evaluated at $V = V_o$) is the equilibrium value of the bulk modulus of the electron gas (B_e). Hence, $U = (p/2)\Phi + B_e(V/V_o)^m/(m(m-1))$, where p is the number of nearest-neighbour atoms surrounding a central atom. As the basic conclusions of the analysis do not depend on this approximation, we ignore core exclusion, exchange, and correlation effects, and approximate B_e by the bulk modulus due to the kinetic energy of the electron gas (so that m is $-2/3$)[24–26]. Following the approach used by Thomas[24], calculating the derivatives for elastic stiffnesses and applying the condition for equilibrium ($\delta U/\delta V = 0$ for $V = V_o$) results in $C_{11} - C_{12} = 2B_e(1-m)^{-1}$, $C_{44} = (a^2\Phi'' + 2B_e(1-m)^{-1})/3$, and $C_{11} + 2C_{12} = a^2\Phi'' + B_e(1-3m)(1-m)^{-1}$ for b.c.c. phases and $C_{11} - C_{12} = (a^2\Phi'' + 7B_e(1-m)^{-1})/4$, $C_{44} = (a^2\Phi'' + 3B_e(1-m)^{-1})/4$, and $C_{11} + 2C_{12} = a^2\Phi'' + B_e(1-3m)(1-m)^{-1}$ for f.c.c. phases, where Φ'' is $d^2\Phi/dr^2$ evaluated at the equilibrium interatomic separation $r = r_o$ and where a is the lattice parameter. These equations are substituted into equations (1) and (2) to obtain $\nu(110, 1\bar{1}0)$ and $\nu(110, 001)$ as a function of only $B_e/(a^2\Phi'')$. For nearly vanishing values of B_e, these equations provide minimum and maximum Poisson's ratios of −1 and 2 for b.c.c. and 0 and 1/2 for f.c.c. Simple geometrical arguments, which are illustrated in Fig. 3 for b.c.c., explain why nearest-neighbour central forces result in a negative Poisson ratio for b.c.c. phases, but not for f.c.c. or h.c.p. phases.

In Fig. 1b we compare the relationship between $\nu(110, 1\bar{1}0)$ and $\nu(110, 001)$ obtained from theory and experiment for b.c.c. phases. Considering the simplicity of this theory and the absence of any adjustable parameters, the agreement is quite good. Also, Fig. 1a shows that the theoretically predicted dependence of $\nu(110, 1\bar{1}0)$ and $\nu(110, 001)$ on $[B_e/(a^2\Phi'')]^{2/5}$ is quite similar to the experimentally determined variation of these Poisson's ratios with work function. These dependent variables were chosen for comparison of theory and experiment because free-electron theory predicts that $B_e^{2/5}$ is proportional to the Fermi energy (E_F), and the work function (W_F) differs in magnitude from E_F by only the contribution from surface dipoles. Hence increasing W_F increases the bulk modulus contribution from the electron gas. The above equations for b.c.c. metals imply that the auxetic behaviour disappears as the mechanical anisotropy becomes small, which is consistent with observations[21]. However, other types of structures are known that are both auxetic and isotropic[14].

Comparison of the theoretical and observed dependence of the Poisson's ratios on work function for f.c.c. metals (Fig. 2) indicates

qualitatively similar trends. But although the model predicts for b.c.c. that $\nu(110, 1\bar{1}0)$ approaches −1 and $\nu(110, 001)$ approaches 2 as B_e vanishes, the corresponding calculated Poisson's ratios for the f.c.c. phases are 0 and 1/2, respectively. Hence, the present simplified theory must be modified for the f.c.c. metals by the inclusion of interatomic potential or band-structure effects that can be expressed as many-body forces. Evidence that such forces cannot be ignored for f.c.c. metals is provided by Cousins and Martin[27], who show that the crystal potential for f.c.c. metals like Cu, Ag, Au and Ni cannot be reliably expressed as the sum of pairwise interatomic and volume-dependent terms. Inclusion of many-body forces can shift the Poisson's ratios downwards to approximately the observed values. For example, application of the simple three-atom, Born–Mayer-type potential of Cousins[28] provides limiting values of $\nu(110, 1\bar{1}0) = -1$ and $\nu(110, 001) = 2$, which are identical to the results for b.c.c. phases that are described by the pairwise interaction model. As for the case of b.c.c. phases, such large-magnitude Poisson's ratios are reduced by the effect of the electron-gas bulk modulus, which increases with increasing work function.

Based on these results we make the following conclusions. Pairwise central forces can explain the large negative values of $\nu(110, 1\bar{1}0)$ and the large positive values of $\nu(110, 001)$ for the b.c.c. metals. An increasing electron-gas contribution to bulk modulus with increasing work function, which helps stabilize the b.c.c. phases as an energy minima, simultaneously makes $\nu(110, 1\bar{1}0)$ less negative and $\nu(110, 001)$ less positive. The dependence of $\nu(110, 1\bar{1}0)$ and $\nu(110, 001)$ on work function is similar for the f.c.c. and b.c.c. metals. However, significant auxetic behaviour for the f.c.c. metals depends on the existence of a substantial many-body contribution to the binding energy. The present analysis indicates that Poisson's ratios of $\nu(110, 1\bar{1}0) = -1$ and $\nu(110, 001) = 2$ can be closely approached by either f.c.c. or b.c.c. phases that have negligible electron-gas contributions—although precisely reaching these values results in a soft mode shear instability. The above conclusions from theory and experimental results are opposite to the previous suggestion[21] that the electron-gas contribution causes negative Poisson's ratios.

The existence of negative Poisson's ratios for the cubic metals has practical importance, especially as a negative Poisson's ratio reverses the compensation effects of positive Poisson's ratios on the volume and area changes caused by a uniaxial stress. One example is a method for obtaining over a two-fold increase in the sensitivity of a strain sensor by sandwiching a sheet of piezoelectric polymer between two thick auxetic metal electrodes. This sensitivity increase occurs because the negative Poisson's ratio of the metal electrode amplifies the effect of an applied in-plane uniaxial strain on sensor sheet area.

Some types of applications previously proposed for axially auxetic materials[3,4] are also possible for the non-axially auxetic cubic metals. The prospects for such applications are enhanced by the commercial availability of non-axially auxetic metals as large single crystals. For example, large single crystals of Ni_3Al, which has[18] a minimum Poisson's ratio of −0.18, are used as vanes for aircraft gas turbine engines[29]. □

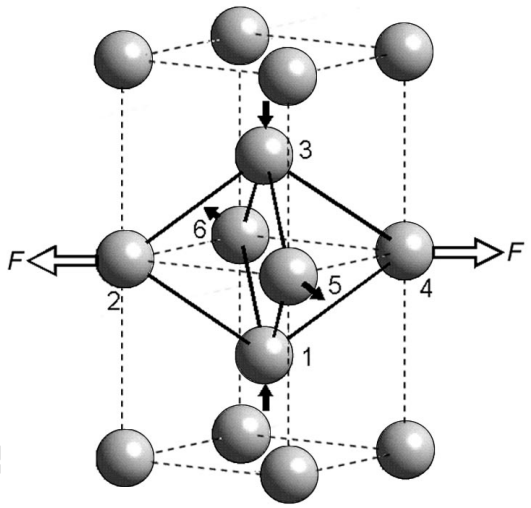

Figure 3 The structural origin of a negative Poisson's ratio and a giant positive Poisson's ratio for the case of a rigid-sphere b.c.c. solid. The solid minimizes density decrease during deformation by maintaining intersphere contact. Two b.c.c. unit cells (defined by the dotted lines) provide a crystallographic reference for describing the relative directions of atomic displacements (black arrows) of atoms 1–6 in response to an applied force in the [110] direction (*F*, indicated by the two white arrows). Decreasing the acute angle in the rhombus defined by atoms 1–4 is the only way to elongate the crystal in the [110] stress direction without increasing the nearest-neighbour separations (indicated by the solid black lines). Hence, the separation between atoms 1 and 3 decreases, providing a positive $\nu(110, 001)$. This angle decrease partially closes this rhombus, thereby pushing atoms 5 and 6 apart (corresponding to a negative $\nu(110, 1\bar{1}0)$). Simple geometrical analysis of these deformations provides that $\nu(110, 001) = 2$ and $\nu(110, 1\bar{1}0) = -1$. Similarly, simple pictures indicate that the minimum Poisson's ratio is zero for rigid-sphere f.c.c. and h.c.p. phases. Atoms in next-nearest-neighbour $(1\bar{1}0)$ sheets are orthogonally in contact for f.c.c. Hence, the dimension in the $[1\bar{1}0]$ direction is unaffected by a [110] strain and $\nu(110, 1\bar{1}0) = 0$. Likewise, an infinitesimal uniaxial elongation orthogonal to a close-packed plane of rigid-sphere atoms in h.c.p. cannot significantly affect packing in this plane, so the minimum Poisson's ratio is zero.

Received 7 April; accepted 1 December 1997.

1. Keskar, N. R. & Chelikowsky, J. R. Negative Poisson ratios in crystalline SiO_2 from first-principles calculations. *Nature* **358,** 222–224 (1992).
2. Gibson, L. J., Ashby, M. F., Schajer, G. S. & Robertson, C. I. The mechanics of two-dimensional cellular materials. *Proc. R. Soc. Lond. A* **382,** 25–42 (1982).
3. Lakes, R. S. Foam structures with a negative Poisson's ratio. *Science* **235,** 1038–1040 (1987).
4. Evans, K. E., Nkansah, M. A., Hutchinson, I. J. & Rogers, S. C. Molecular network design. *Nature* **353,** 124 (1991).
5. Rothenburg, L., Berlin, A. A. & Bathurst, R. J. Microstructure of isotropic materials with negative Poisson's ratio. *Nature* **354,** 470–472 (1991).
6. Yeganeh-Haeri, A., Weidner, D. J. & Parise, J. B. Elasticity of α-cristobalite—a silicon dioxide with negative Poisson's ratio. *Science* **257,** 650–652 (1992).
7. Wei, G. & Edwards, S. F. Polymer networks with negative Poisson's ratios. *Comput. Poly. Sci.* **2,** 44–54 (1992).
8. Baughman, R. H. & Galvão, D. S. Crystalline networks with unusual predicted mechanical and thermal properties. *Nature* **365,** 735–737 (1993).
9. Smith, W. A. in *Proc. 1991 Ultrasonics Symp.* (ed. McAvoy, B. R.) 661–666 (*IEEE*, Piscataway, NJ, 1992).
10. Wojciechowski, K. W. Two-dimensional isotropic solid with a negative Poisson's ratio. *Phys. Lett. A* **137,** 60–64 (1989).
11. Lakes, R. S. No contractile obligations. *Nature* **358,** 713–714 (1992).
12. Miki, M. & Morotsu, Y. The peculiar behavior of the Poisson's ratio of laminated composites. *JSME Int. J.* **32,** 67–72 (1989).
13. Lakes, R. S. Deformation mechanisms of negative Poisson's ratio materials: structural aspects. *J. Mater. Sci.* **26,** 2287–2292 (1989).
14. Milton, G. W. Composite materials with Poisson's ratios close to −1. *J. Mech. Phys. Solids* **40,** 1105–1137 (1992).
15. Turley, J. & Sines, J. The anisotropy of Young's modulus, shear modulus and Poisson's ratio in cubic materials. *J. Phys. D* **4,** 264–271 (1971).
16. Milstein, F. & Huang, K. Existence of a negative Poisson ratio in fcc crystals. *Phys. Rev.* **19,** 2030–2033 (1979).
17. Li, Y. Anisotropic behavior of Poisson's ratio, Young's modulus, and shear modulus in hexagonal materials. *Phys. Status Solidi A* **38,** 171–175 (1976).
18. Every, A. G. & McCurdy, A. K. in *Landolt-Börnstein* (ed. Nelson, D. F.) 11–133 (New Ser. III/29a, Springer, Berlin, 1992).
19. Gunton, D. J. & Saunders, G. A. The Young's modulus and Poisson's ratio of arsenic, antimony, and bismuth. *J. Mater. Sci.* **7,** 1061–1068 (1972).
20. Fioretto, D. *et al.* Brillouin-scattering determination of the elastic constants of epitaxial fcc C_{60} film. *Phys. Rev. B* **52,** R8707–R8710 (1995).
21. Jain, M. & Verma, M. P. Poisson's ratios in cubic crystals corresponding to (110) loading. *Ind. J. Pure Appl. Phys.* **28,** 178–182 (1990).
22. Grigoriev, I. S. & Meilikhov, E. Z. (eds) *Handbook of Physical Properties* Ch. 25, 697–698 (CRC Press, New York, 1997).
23. Miedema, A. R., de Châtel, P. F. & de Boer, F. R. Cohesion in alloys—fundamentals of a semi-empirical model. *Physica B* **100,** 1–28 (1980).
24. Thomas, J. M. Failure of the Cauchy relation in cubic metals. *Scripta Metall.* **5,** 787–790 (1971).
25. Gilman, J. J. Bulk stiffnesses of metals. *Mater. Sci. Eng.* **7,** 357–361 (1971).
26. Ashcroft, N. A. & Mermin, N. D. *Solid State Physics* Ch. 2, 30–55 (Holt, Reinehardt & Winsten, New York, 1976).
27. Cousins, C. S. G. & Martin, J. W. Extended Cauchy discrepancies—measures of non-central, non-isotropic interactions in crystals. *J. Phys. F* **8,** 2279–2291 (1978).

28. Cousins, C. S. G. Evidence for short range, three-body interactions in copper. *J. Phys. F* **3,** 1915–1920 (1973).
29. Nakamura, M. Fundamental properties of intermetallic compounds. *Mater. Res. Soc. Bull.* **XX(8),** 33–39 (1995).

Supplementary Information is available on *Nature*'s World-Wide Web site (http://www.nature.com) or as paper copy from Mary Sheehan at the London editorial office of *Nature*.

Acknowledgements. We thank R. S. Lakes, J. J. Gilman, L. W. Shacklette, R. C. Morris, and S. O. Dantas for important comments.

Correspondence and requests for materials should be addressed to R.H.B. (e-mail: ray.baughman@alliedsignal.com).

Voltage-dependent anchoring of a nematic liquid crystal on a grating surface

G. P. Bryan-Brown, C. V. Brown, I. C. Sage & V. C. Hui

Defence Evaluation and Research Agency, St Andrews Road, Malvern, Worcestershire WR14 3PS, UK

The switching properties of most liquid-crystal electro-optic devices rely mainly on the reorientation of the average molecular direction (director) within the bulk of the liquid-crystal layer[1]. Reorientation of the director at or near the surfaces of the layer usually has an insignificant effect on device performance. Here we describe a different configuration in which a nematic liquid crystal is placed between a flat surface treated to induce a parallel anchoring of the director and a grating surface treated to give a perpendicular anchoring. We show that this configuration leads to an effective azimuthal anchoring at the grating surface that depends on the applied voltage when the nematic phase has negative dielectric anisotropy (that is, the director has a tendency to align perpendicular to the applied field). This leads to a voltage-controlled twist effect in the liquid-crystal cell that is highly sensitive to the grating profile. Furthermore, this twist effect possesses an electro-optic response which is far less dependent on viewing angle compared to many other liquid-crystal display configurations. We therefore suggest that this technology might find application in the next generation of liquid-crystal displays.

Liquid-crystal displays consist of a liquid-crystal layer contained between two substrate surfaces. These surfaces impose a preferred orientation of the liquid-crystal director to generate uniform optical properties. Treating the surface with a low-surface-energy surfactant[2] leads to perpendicular alignment (director orthogonal to surface plane) whereas an ordered polymer coating leads to planar alignment (director in surface plane with preferred direction). Planar alignment is usually achieved using a polymer which has been ordered by rubbing with a nylon cloth[3], although prototypes are now emerging in which the ordering is induced optically[4]. The earliest alignment method to be explained quantitatively is that in which a grating surface is used[5]. The liquid-crystal director aligns along the grating grooves in order to minimize the elastic distortion energy.

Here we consider a nematic liquid crystal in contact with a grating surface which has been treated with a low-energy surfactant. Such a treatment constrains the director to align perpendicular to the local surface direction. The average director orientation is then perpendicular to the average surface direction for a symmetric grating profile. If the liquid crystal has negative dielectric anisotropy, then application of a sufficient electric field will lead to a planar configuration in which the director lies along the grating grooves. This is also well known. However, in the present work the grating surface is placed opposite a normally planar surface in which the planar anchoring direction is perpendicular to the grating groove direction. A new mode of operation is then observed. Figure 1 shows a schematic view of the behaviour of this configuration in which the grating grooves are in the y direction (that is, out of the plane of the figure) and the planar anchored direction is along the x axis. The director is represented by the black rods. When no voltage is applied between the substrates ($V = 0$), the director has a tilt in the x–z plane which varies roughly linearly with z. When the voltage is raised to V_1, the tilt angle decreases because the applied field couples to the negative dielectric anisotropy but the director remains in the x–z plane as this is the preferred anchoring direction on the planar surface. However, when the voltage is increased the liquid-crystal tilt is lowered in the vicinity of the grating surface which then starts to impose an azimuthal twisting torque on the near-surface director. Eventually, at a sufficient voltage (V_2), the twist torque overcomes the bulk twist threshold energy and a finite twist is observed. These energies may be compared as follows. The maximum twist torque which can be imposed by the grating is given by[5]

$$W_\phi = \frac{1}{4}\sqrt{k_{11}k_{33}}a^2\left(\frac{2\pi}{L}\right)^3 \quad (1)$$

where a and L are respectively the amplitude and pitch of a sinusoidal oscillation, and k_{11} and k_{33} are the liquid-crystal elastic constants. For a typical grating with an amplitude of 0.25 μm and a pitch of 1 μm, this energy is roughly 4×10^{-5} J m^{-2}. The twist threshold energy is given by k_{22}/d where d is the cell gap. For a 5-μm cell this energy is typically only 1×10^{-6} J m^{-2}. Therefore in the high-voltage regime, the grating alignment energy dominates over the twist energy and the cell is expected to have a 90° twist as shown in Fig. 1 at $V = V_2$. This configuration thus allows a voltage-controlled twist (VCT) effect.

The VCT behaviour can also be numerically analysed using a finite-element approach in which a grid of directors are elastically coupled to each other and contained between surfaces with defined boundary conditions. For a particular applied voltage, the system is relaxed until the minimum energy is found. Figure 2a shows an example of a predicted configuration at 0 V. In this case, the liquid crystal is continuously distorted between the planar boundary condition on the top flat surface and the perpendicular boundary condition on the bottom grating surface. If the voltage is set to 15 V (Fig. 2b), the cell relaxes into a configuration with lower average tilt in which the director near the grating is twisted out of the x–z plane (represented by shorter lines). Therefore this approach also predicts a VCT effect.

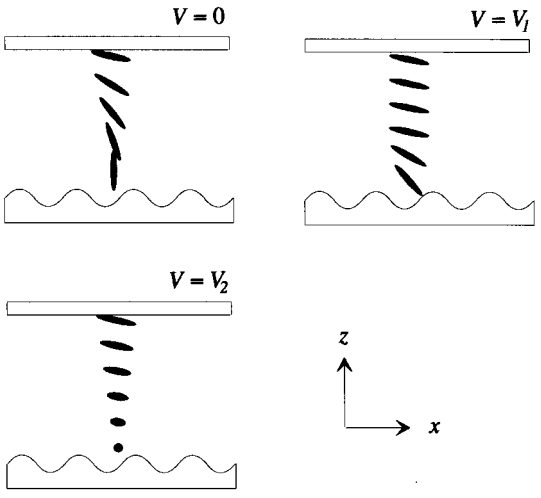

Figure 1 Schematic representation of the liquid-crystal cell geometry used to observe the VCT effect. Details are given in the text.